Western Engineering

MSE 4499 — Mechatronic Design Project

Fruit Picking Robot

by

Alexander Cleator

Ziqin Shang

Qi Qi

Mingyang Xu

Final Report

Faculty Advisor: Prof. L. Brown

Date Submitted: Friday April 3, 2020

Word Count: 7942

Contents

Table of Figures

Table of Tables

Executive Summary

In this summative report, the entire design process is outlined and discussed for the development of a fully autonomous tomato harvesting mobile robot to supplement a substantial worker shortage in the agricultural industry. The function of the device is to autonomously navigate a tomato or cherry tomato greenhouse, and identify, pick, and collect tomatoes. This task was decomposed into several subsystems, navigation, image processing, robotic manipulation, and the robot-tomato interface. Speed and accuracy tests were conducted were conducted on the relevant systems which resulted in the successful iterative development of these systems. Several comprehensive progress reviews were conducted during which the current progress was discussed as was suggestions for improvement including the switch from encoder-based navigation to the use of an external sensor (such as a line-tracker). Each of the independent subsystems were successfully developed, however due to current world events (COVID-19 pandemic) several components necessary to finalize the development of the device were not fabricated resulting in a less-than-fully-functional prototype despite promising test data.

Introduction

In 2014, 26,400 agricultural jobs were unfilled according to a study published by the Canadian Agricultural and Human Resources Council funded by the Government of Canada's Sectoral Initiatives program [1]. By 2025, this gap is expected to grow to 113,800. This labour shortage proliferates numerous costs in the agricultural industry, with 55% of respondents claiming production delays, and lost revenue. Other attributed costs include production losses, delayed or cancelled capital expansions, and overtime costs. Aside from the lack of workers available, the same study continues to state that finding quality workers is more important the quantity of applicants. Higher quality workers can be defined as better skilled workers, who have a natural interest in their work resulting in a lower turnover rate and a higher average quality of worker as skills improve over time.

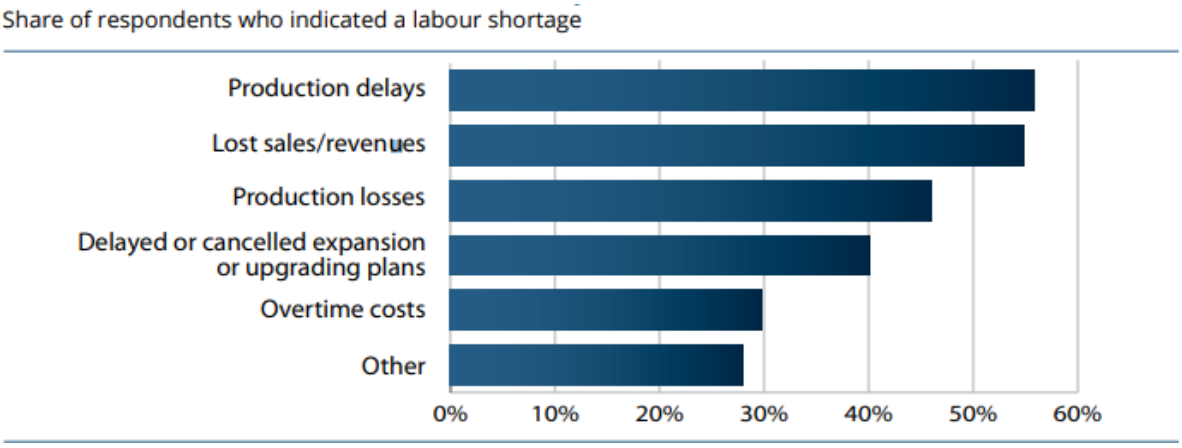

Figure 1: Labour Shortage Consequences

This large-scale labour shortage was estimated to cost farmers a total of $2.9 billion in lost revenue in 2017 according to the Labour Market Forecast to 2029, also published by the Canadian Agricultural Human Resources Council. In 2019 Canada's agriculture sector lost $2.9 billion to lost sales because of this tremendous shortage,

and that loss is predicted to grow further [2]. While harvesting labourers are only predicted to make up 7% of the total labour gap, it is a repetitive, labour intensive task, which pays poorly, and is critical to production. Regardless of the potential losses of an unfilled management position, compared to an unfilled general labourer or harvester, the loss that can be attributed to the shortage of harvesters can be conservatively estimated to be at least 3% of the total loss across the agricultural industry. This conservative estimate would suggest $90 million dollars in 2019 (likely more) can be directly attributed to the lack of harvesting positions being filled. Consequently, 30% of respondents stated that they considered overtime costs to be a direct result of the labour shortage as well. Excessive overtime work often results in poor morale among workers, high turnover rates, and poor-quality work [3] [4], which contributes back to the previously stated results of extreme labour shortage. Automating harvesting positions would address most of the above issues, while displacing a minimal number of established jobs, and create new skilled jobs in the manufacturing and automation servicing industries.

The proposed solution is to automate the agricultural harvesting process and create a mechatronic device to identify and pick greenhouse tomatoes. This device would be marketed towards small and medium sized farms, where it would be more cost efficient to have the device work in relative isolation in comparison to large farms with large crews where many people working together would be more efficient. Furthermore, marketing to a smaller market could act as a pilot project, to test the scalability of the concept.

Background Information

Current State of the Art

Automating the fruit picking process is not an entirely novel idea, several prototypes of functional devices have been designed in the past, however they have some critical errors that our team intends to address. It is important to first establish the current state of the art regarding automating soft-fruit harvesting. The most notable example is a very recent development by a UK start-up enterprise called Fieldwork Robotics. Their device is capable of picking 1250 raspberries per hour compared to 1875 a human could pick in that same time period [5]. Their robot uses template-based image processing, and a vaguely described four-armed flexible robotic manipulator. UK based media outlet Express covered the story, and in an interview with Fieldworks' robotics director Dr. Martin Stoelen, he stated "Different light conditions, branches, [and] pests … have been the biggest challenges" in reference to the sensitivity of the image processing methods to debris or partial occlusion of the raspberries. To date, £672,000 ($1,142,000 CAD) have been invested in the project [6]. This project is at the forefront of the current technological frontier regarding fruit-picking automation, highlighting that image processing is the most challenging issue of this endeavor.

In a similar article published in the Washington post, image processing concerns are echoed as the device described is unable to differentiate between ripe, over, or underripe fruit. While outlining the technological concerns regarding the image processing issues, the article further references mechanical brutality towards produce. The focus of the article however is on the social implications of automating fruit

harvesting. There is a clear and obvious stigma towards automation as it is seen as a replacement for human jobs (which to an extend is justified), however the benefits of creating skilled positions are also discussed.

Both articles refer to similar primary problems, and several secondary ones. The primary issues outlined are the image processing considerations, and the robot's ability to safely handle fruit without causing any damage. If a robot is unable to both identify and safely pick fruit, it is essentially useless in this application. As our team lacks an understanding of both the theory and application of advanced image processing techniques such as template matching, for the sake of feasibility our device will locate the centroid and outline of a color blob and cut a prescribed distance above the fruit. The second problem of the safe handling of the produce is a much more feasible task. The secondary problems include increasing the speed of the entire operation, ensuring the device can navigate difficult terrain, and finally can operate outdoors.

Color Blob Image Segmentation

To effectively pick tomatoes off a plant, the tomato must be identified and located using colour blob image processing techniques. This problem can be split into two

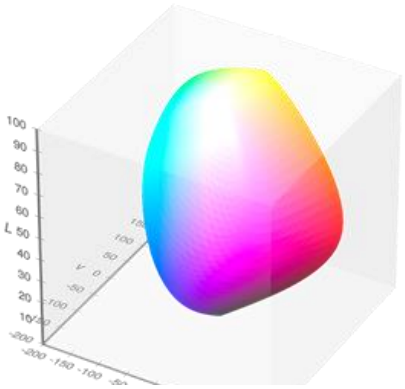

Figure 3: CIE LUV Colour Space

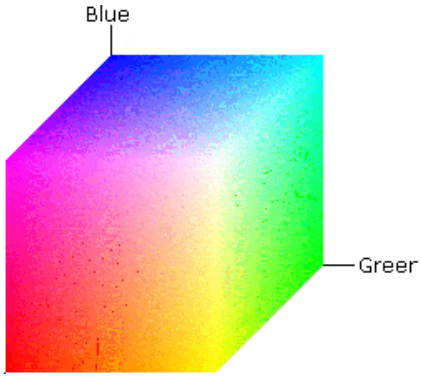

Figure 2:RGB Colour Space

distinct sub-problems. First, the tomato must be isolated from the background, second, the tomato must be assigned a position in three-dimensional space to allow the robotic manipulator to interact with it. Reviewing an IEEE published paper entitled “Color Blob Segmentation by MSER Analysis” [7], color blob image segmentation requires four steps.

First, a set of colour values to be segmented must be defined. Next, the image is converted from RGB colour space (red-green-blue) to the CIE Luv colour space.

Next, the colour value of each pixel must be compared to those next to it. This is achieved by defining a vector to each pixel with values L, u, and v from the Luv colour space (μ), as well as a covariance matrix (Σ) based on Gaussian distributions to determine the colour similarities between pixels. Using these matrices, the Bhattacharyya distance (a quantitative value indicating the similarity of two pixels) can be determined using the following relationship.

Equation 1: Bhattacharyya Distance

$$\beta = \frac{1}{2}\ln\frac{\left|\frac{\vec{\Sigma}_1+\vec{\Sigma}_2}{2}\right|}{\sqrt{\left|\vec{\Sigma}_1\right|\left|\vec{\Sigma}_2\right|}} + \frac{1}{8}(\vec{\mu}_2-\vec{\mu}_1)^t\left[\frac{\vec{\Sigma}_1+\vec{\Sigma}_2}{2}\right]^{-1}(\vec{\mu}_2-\vec{\mu}_1),$$

Finally, a list of Bhattacharyya pixel distances is created, and those beneath a set sensitivity threshold are grouped to form the selected subregion of the image. This process is typically completed by software included in most image processing packages, and likely Matlab. However, it is important to understand the underlying principles of image segmentation, to refine or develop an appropriate algorithm to isolate tomatoes from their background.

Scope, Constraints, and Objectives

Scope

In order to ensure the completion of a functional device, the scope of the project will (in some ways) be limited. This was primarily implemented during the development of concepts, with an obvious example of this being the immediate elimination of any air-borne or UAV (unmanned aerial vehicle) based solutions. These solutions require very precise control, and very tight tolerances in manufacturing which are not feasible with the available budget and resources.

With these limitations, the objective of the project is to develop a fully functional device that can accurately and repeatedly pick tomatoes. The final device will be a mobile robot, designed for outdoor use, that can identify tomatoes using machine vision, and autonomously pick them using a robotic manipulator.

Objectives

Fast Response Speed

Smaller sized fruit such as tomatoes can be harvested much faster, less than 20 seconds each (an automatic tomato harvesting machine designed at Beijing University of Technology achieved an operational time of 8 seconds [8]. Our robot aims to reduce their completion times.

Easy and Intuitive to Operate

The machine should be simple to operate, requiring only minimal safety training.

Complex Terrains Functionable

The machine should be able to function on steep terrain with slopes exceeding 50°. Many nurseries and farms, noticeably in China and India include steep terrain. Traditional harvesters are limited to open fields with slopes under 30 [9]. The ability to operate on steep, and uneven terrain would greatly improve the machines versatility.

Cost Efficient

The cost of the device should be minimized.

Integrable to Larger System

The machine should be integrable into a complete fruit harvesting process that also includes fruit cleaning, grading, disinfection, artificial waxing etc.

Constraints

Multiple Degrees of Freedom Movement

At least four degrees of freedom of movement are required to allow for multiple possible position configurations to avoid obstacles such as foliage.

Durable and Maintainable

Sensitive electronic components must be protected and made replaceable, most mechanical components must be interchangeable and repairable. Many farms are in remote areas and are not easily accessible by support technicians. Modern farm equipment is dependent on electronics (which are often difficult or impossible to repair without a qualified technician) which can cause delays in case of repairs.

Safe to Operate

The machine should meet Occupational Health and Safety Act (OHSA) standards, other related regulations and local laws.

Safe for Greenery

The core advantage of an automatic harvester over mechanical harvesters such as lime shakers, air blasters, and canopy shakers is that it does not damage the trees or fruits. To preserve this fundamental advantage is imperative.

Weather and Dust Proof

The machine is expected to work outdoors under various conditions.

Fail Safe

The device must fail such that nearby workers are not injured.

Accurate Fruit Detection

The implemented fruit detection method should be able to identify fruit from a noisy background, returning 3D coordinates to the processor. The fruit detection method should work under various scenarios, including insufficient illuminance, strong light intensity (such as at noon), movement, and partial occlusion.

Concept Generation and Selection

During the concept generation and selection process, a series of design techniques were implemented, including functional decomposition, morphological analysis and the use of a decision matrix. In this section, each generated concept will be explained, optimal solutions will be discussed, and a comprehensive solution will be provided.

Functional decomposition

After analyzing the given constraints and objectives, to build a functional fruit-picking robot, the following functions must be completed:

• Driving mechanism: The robot must move freely

• Picking mechanism: The robot must pick tomatoes

• Detaching mechanism: The robot must detach the tomatoes from their vine

• Collecting mechanism: The robot must store the collected tomatoes

• Machine vision: The robot must locate the tomatoes

Morphological Analysis

There are various ways to achieve above functions, after group brainstorming and researching, multiple possible solutions for each subsystem were generated.

Moving Subsystem

1. Four wheels

This method is the simplest to implement, requiring four wheels that have high coefficients of static friction to ensure the robot can travel over unpaved surfaces. The advantage of this concept is that four wheels allow the robot to maneuver easily. The disadvantage is the associated cost and it may not be able to operate on rough terrain.

2. Caterpillar tracks

Caterpillar tracks provide far more traction than wheels over unpaved surfaced. Two motors are used to drive the tracks, with a large gear to provide torque, and a pinion for tensioning.

3. Multi-Legged

A complex multi-legged walker can climb and travel over obstacles. Multiple stepper motors, and complex linkages will be used to implement this mechanism, adding significant complexity. The advantage is that it can travel easily on rough surfaces, the disadvantage is its cost and complexity.

4. Rail

A railway system could be constructed on the ground for the robot to travel on. This method is very simple but not cost-efficient. Although it is very easy to operate, a railway system would have to be built throughout the operating environment, which is very expensive. Additionally, the distance between the robot and the plant is fixed, so the robot may be too far or too close to the plant to operate properly.

Picking Subsystem

To pick up an object in three-dimensional space, a robotic arm is the optimal solution because it has six degrees of freedom. The following mechanisms will be implemented on a robotic manipulator.

1. Clamp

The simplest possible solution, however, the stem needs to be cut to detach the fruit from the plant. A detachment mechanism would be implemented. To facilitate force control, a closed-loop control system is required for this mechanism to operate.

2. Small basket

This mechanism is a small basket with a detachment mechanism above. The robot will detect the tomato, place the basket below it, then the detachment mechanism cuts the stem. This method does not require a force control system.

3. Vacuum

Using a vacuum to collect the desired tomato can easily damage it. Furthermore, it can be quite expensive, and complex to implement properly. This solution requires significant power, which would result in high operating costs.

4. Transmission tube

This method of collecting the fruit is to cut the stem, then allow the fruit to fall down a flexible rubber or PVC tube. This is the easiest, and most cost-effective way to transport tomatoes.

Detaching Subsystem

1. Scissor

A pair of scissors will be attached to the picking mechanism to cut the stem above the fruit.

2. Knife

A knife is connected to a stepper motor. After identifying the location of the stem, the knife will pass through that location to cut the stem. However, the blade may damage the plant.

3. Saw

A motor is connected to a saw blade. After identifying the location of the stem, the saw will pass through that location to cut the stem. This method has the same disadvantage as the knife, as it may damage the fruit.

Collection Subsystem

1. Basket

2. Case

3. Net

The previous three collection mechanisms are all considered as viable and effective solutions.

Concept Selection

Go/No-Go Screening

Driving Subsystem

For the driving subsystem, the objectives that will be evaluated are:

Complexity: Difficulty to implement, test or operate

Maneuverability: Difficulty to change direction during operation

Cost: The value of money to manufacture

Safety: The level of danger inherent to operators

Durability: The ability to remain functional without excessive maintenance or repair

Reliability: The capacity to perform as required over time

Table I: Movement Subsystem Go/ No-Go Matrix

	Complexity	Maneuverability	Cost	Safety	Durability	Reliability	Result
Four wheels	GO	GO	GO	GO	GO	GO	GO
Caterpillar bands	GO	GO	GO	GO	GO	GO	GO
Multi-Legged	NO-GO	GO	NO-GO	GO	GO	GO	NO-GO
Rail	GO	NO-GO	NO-GO	GO	GO	GO	NO-GO

Picking Subsystem

For the picking subsystem, the objectives that will be evaluated are as follows:

Complexity, Cost, Durability and Reliability: Same as above

Adaptability: Ability to pick different types or size of fruit

Safety to plants: The level of inherent danger to plants

Table II:Tomato Picking Subsystem Go/ No-Go Matrix

	Complexity	Adaptability	Cost	Safety to plant	Durability	Reliability	Result

Clamp	GO	NO-GO	GO	NO-GO	GO	GO	NO-GO
Basket	GO	GO	GO	GO	GO	GO	GO
Vacuum	GO	GO	GO	GO	GO	GO	GO
tube	GO	GO	GO	GO	GO	GO	GO

Detaching Subsystem

For the detaching subsystem, the objective that will be evaluated is its safety towards plants

Table III: Tomato Detachment Subsystem Go/ No-Go Matrix

	Safety to Plant	Result
Scissor	GO	GO
Knife	NO-GO	NO-GO
Saw	NO-GO	NO-GO

Collection Subsystem

All collecting methods are viable.

Decision Matrix

To select the optimal solution from the above generated concepts, a decision matrix will be used. The decision matrix will be evaluated based on different criterial corresponding weights will be assigned to each of the following:

Complexity (Weight=3): Difficulty to implement, test or operate

Cost (Weight=5): The value of money to produce

Efficiency (Weight=5): The ability to quickly achieve the desired result

Sustainability (Weight=3): The concept's environmental impact

Durability (Weight=4): The ability to remain functional without excessive maintenance or repair

Safety (Weight=4): The level of inherent danger to operators

Reliability (Weight=3): The capacity to perform as required over time

Adaptability (Weight=5): Ability to pick different types or size of fruit

Maneuverability (Weight=5): Difficulty to change direction during operation

Safety to plant (Weight=5): The level of inherent danger to plants

Table IV:Comprehensive Subsystem Decision Matrix

		Complexity	Cost	Efficiency	Sustainability	Durability	Safety
Collecting Subsystem	Net	5	5	3	2	3	3
	Case	4	3	5	3	5	5
	Basket	4	4	4	3	3	3
Detaching Subsystem	Scissor	4	5	5	4	5	5
Picking Subsystem	Tube	4	4	5	4	4	4
	Vacuum	2	1	2	3	1	1
	Basket	4	5	3	4	4	4
Moving Subsystem	Caterpillar Bands	4	4	3	4	5	5
	Four Wheels	4	4	5	4	4	5
Weight		3	5	5	3	4	4

3	N/A	N/A	N/A	94
5	N/A	N/A	N/A	116
4	N/A	N/A	N/A	97
5	N/A	N/A	4	149
5	4	N/A	5	161
1	5	N/A	5	91
5	3	N/A	4	146
5	N/A	2	N/A	124
4	N/A	5	N/A	142
3	5	5	5	
Reliability	Adaptability	Maneuverability	Safety to plant	Total

Design Validation

Frame Analysis

The frame is made from extruded 1060 aluminum alloy beams, 1060 Aluminum is a strong, lightweight material that suitable for various applications, in this application, the frame will be supporting an approximate weight of 5 kg of fruit and 10 kg of robot self-weight.

An FEA analysis was conducted with a loading scenario of 50N distributed force on the base plate which simulates the approximate weight of 5kg, to ensure the accuracy of the test, a fine mesh was used in this analysis with an element size of 8.62mm. The results of the FEA analysis are shown in the following figures.

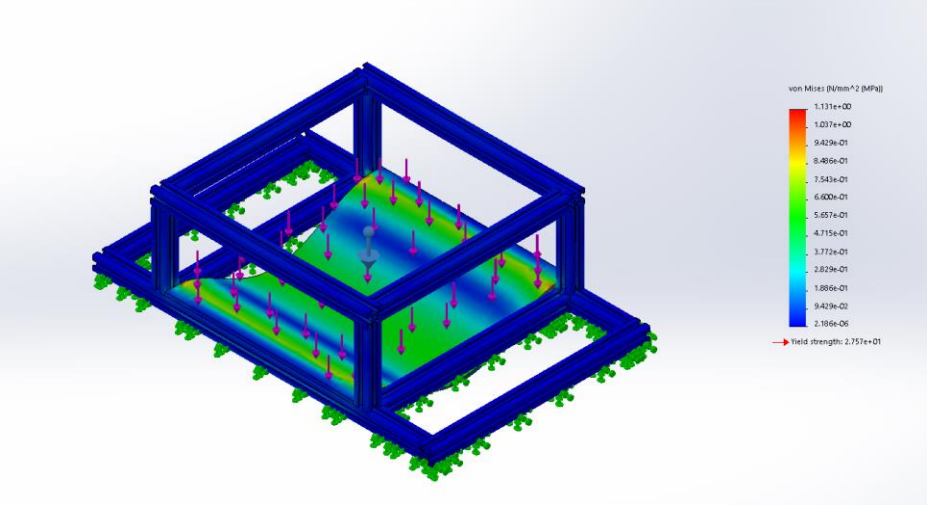

Figure 4: FEA Analysis: Von Mises Stress

It was found that the maximum Von Mises stress occurs on the contact edge of the plate and the frame, which is 1.131 MPa, the yield strength of H12 tempered 1060 aluminum is approximately 76 MPa, indicating no risk of failure by yielding. Furthermore, 1060 aluminum is resistant to corrosion. [10]

The resultant displacement from the same analysis is shown below; it was found that the maximum displacement of 0.015mm occurred along the center line of the plate.

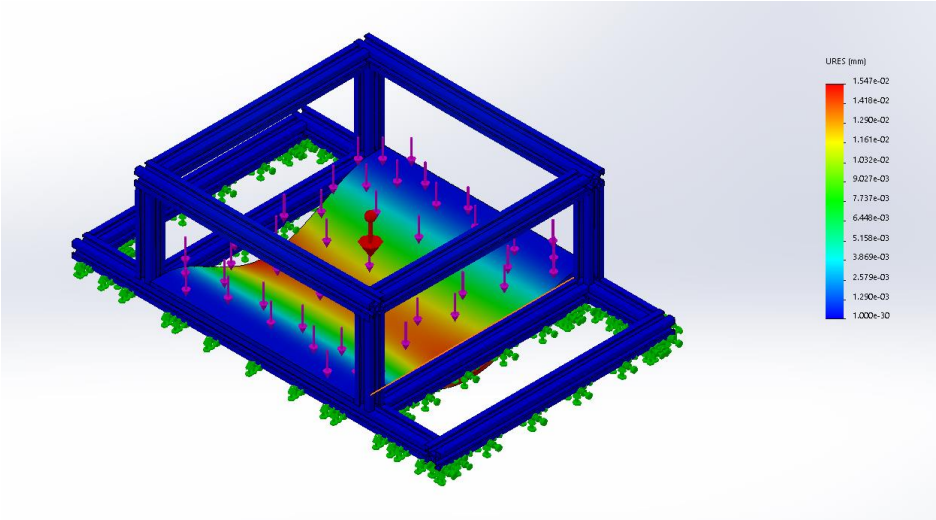

Figure 5: FEA Analysis: Deflection

Motor Analysis

After measuring the weight of the empty robot to be 10kg, and by adding the payload weight of 5kg, the loaded robot will have total weight of 15kg. A normal force of 36.75N can be applied to each of the four wheels. Assuming the frictional coefficient between the rubber wheels and a dry concert ground is 0.6, a frictional force of 22.05N must be overcome. Based on Newton's second law, a net force of 1.5N must be applied to allow the 15kg device to accelerate at a rate of $0.1\frac{m}{s^2}$.

$$F = ma = (15kg)\left(\frac{0.1m}{s^2}\right) = 1.5N$$

Disregarding the moment of inertia of the wheel (as it was determined to be inconsequential), the required torque for 0.1 $\frac{m}{s^2}$. can be calculated as follows:

$$\tau = F\ x\ r = (22.05N + 1.5N)x\ (0.09m) = 2.12\ N.m$$

Equating the applied force and friction, the required steady-state torque can be determined as follows.

$$\tau = F\ x\ r = (22.05N)x\ (0.09m) = 1.98\ N.m$$

By estimating the operational speed of 0.5 $\frac{m}{s}$, the required rotational speed can be calculated using the diameter of the wheel and the linear speed of the robot:

$$\text{circ.} = \ \pi\text{d} = 0.18\text{m x}\ \pi = 0.565\text{m}$$

$$\text{f} = \frac{\text{v}}{\text{circ}}. = \frac{\frac{0.5\text{m}}{\text{s}}}{0.565\text{m}} = 0.884\ \text{Hz}$$

$$\text{f}_{\text{rpm}} = 60\text{f} = 60(0.884) = 53\ \text{rpm}$$

Considering the limited budget, a brushed DC motor is the optimal solution.

In this application, a gearbox is required due to of the high speed, low torque output from the motor.

Based on the specification that the selected motor must have a stall torque over 2.1 Nm and a rated torque ideally as close as possible to 2Nm to maximize mechanical efficiency, a gearbox motor with the following properties was selected.

Voltage	No-load speed	Rated speed	Rated torque	No-load current	Rated current	Stall current
24V DC	172±15 RPM	122 ± 10 RPM	2.5N.m	0.3A	2.3A	7A

The motor has an integrated 1:51 gear reducer, which amplifies the rated torque from 50mNm to 2.5Nm that will fulfill the design requirement. A CNC machined steel shaft mount with an integrated bearing was also purchased to mount the motor on the chassis. A 180mm diameter wheel with aluminum wheel hub and rubber tire will be attached to the motor assembly. The motor can be controlled using pulse width modulation. After a series of tests, a 15VDC supply, operating at a 30% duty cycle could achieve the specified rate of $0.5\frac{m}{s}$. A peak speed of $1.7\frac{m}{s}$ was observed during testing, which would be implemented if not for safety considerations. For this device, rear differential steering was used due to the potential for zero-turn-radius steering. After completing the concept generation and selection phases of the design development, construction began on both a physical prototype and a Solidworks assembly to model the completed concept.

Image Processing Analysis

The image processing system has multiple stages of processing. The steps are presented below:

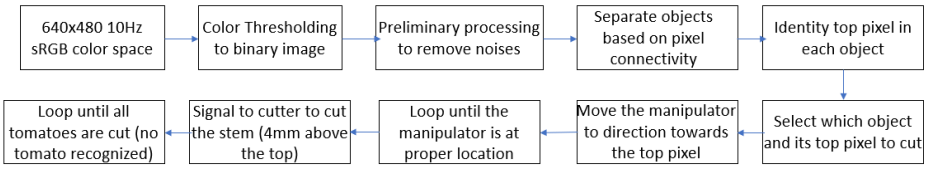

First, the RGB channels are combined into grayscale. Since tomatoes are saturated red with a mix of green, brown (red + green) and blue-sky background, a linear algorithm that promotes red and demotes green and blue was used to create a grayscale image.

$$\text{Grayscale} = 3 * \text{red channel} - 2 * (\text{blue channel} + \text{green channel})$$

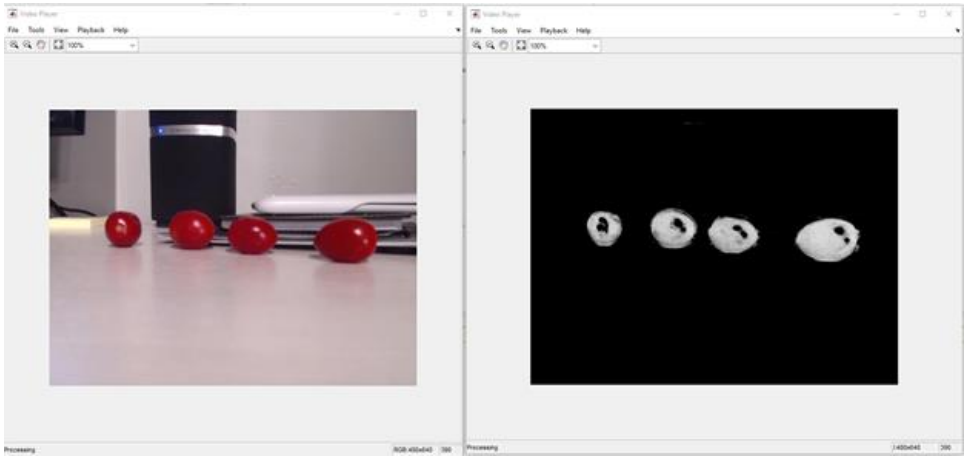

Figure 6: First Iteration Colour Segmentation

Complex lighting conditions often cause noises in the image and color thresholding to create binary image is further exaggerating the problem. Therefore, some techniques are used to remove these noises. As seen in Figure 6: First Iteration Colour Segmentation the holes inside the tomatoes are from overexposure areas due to the point light in the test environment. Filling the contour is required in later processing. To get a cleaner image and fill the hole, morphological reconstruction is used on the image to fill the small gaps and holes as shown in Figure 7: Tomato Segmentation with Closed Contours.

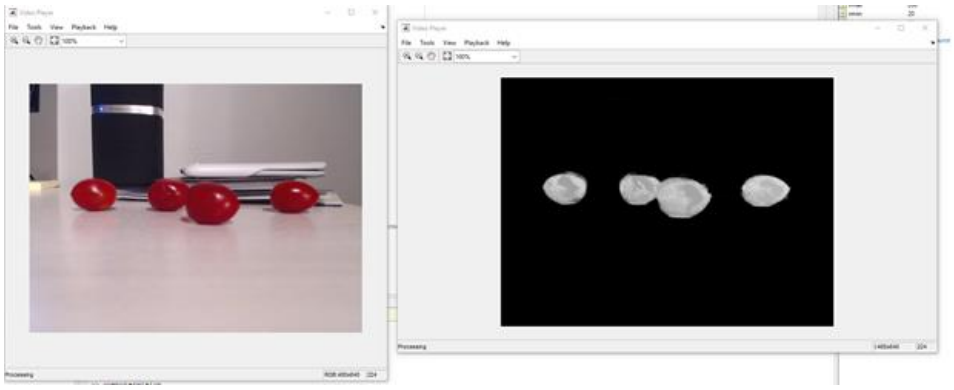

Figure 7: Tomato Segmentation with Closed Contours

After removing overexposed spots, groups of pixel number fewer than 20 are removed to solve the “salt and pepper” type of noise. After obtaining a cleaner image, objects are separated by their pixel connectivity and unique numbers are assigned to each pixel group to identify each tomato. The MATLAB image processing command “bwlabel” is used to assign matrix numbers and to return the total number of objects.

To identify to the stem location, image objects are separated by their regions and each region is individually processed to find the top location of that object. MATLAB’s “find” command is used to return the top location (in the matrix) of each unique object. Each location is determined based on its position relative to the surrounding area. The relative location of selected pixel is compared to the location where the camera is pointing at, the difference is used to command where the end effector should move to. The process continues until there are no more identified tomatoes and their top pixels are presented in the image. Using this procedure, all tomatoes can be identified and cut in sequence.

This traditional image processing technique works well in relatively simple environments. In later development of the actual product, it would be best to combine traditional image processing with machine learning to work in more complex environments. In this case, traditional image processing would be used to deblur or remove noise, machine learning could act as a more robust method of identifing the tomatoes.

Voice Recognition Analysis

The voice recognition system has three stages to process captured sound. The first stage is to down sample the audio captured by the microphone. The second stage is a bandpass filter to reduce surrounding noises. The third stage is TensorFlow based machine learning to recognize the audio.

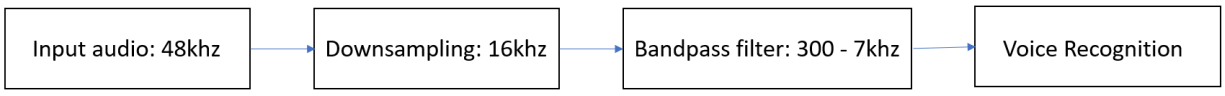

The microphone audio sampling rate is fixed 48khz, however the TensorFlow model is trained on 16khz samples. As 48kHz is three times the 16kHz, to match the 16khz test signal, the recorded sample frequency is reduced by a factor of three.

A bandpass filter of 300Hz – 7kHz is implemented to reduce the surrounding noises. It is found that pronunciation frequency of most western words lay in between 500Hz – 5000 Hz range. The goal of this voice recognition is to recognize a recorded “Stop” sound. First a fast Fourier transformation is performed on the “Stop” sound to analyze the harmonic spectrum.

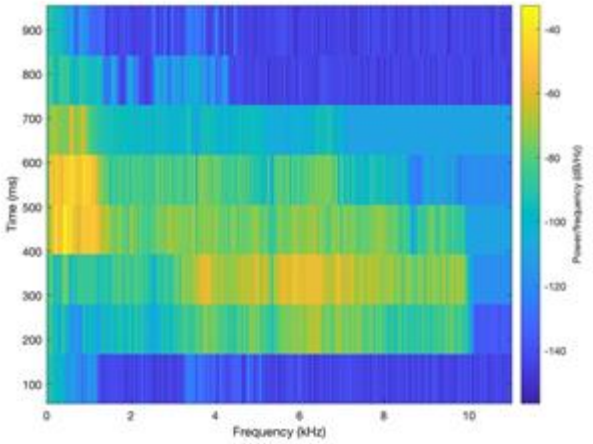

This spectrogram shows that the “s” from “stop” has most energy around 7k Hz range, the “top” sound has frequency expanding between 300 – 1k Hz range. Therefore, 300 – 7k Hz band filter is chosen. A Kaiser window FIR band pass filter is eventually implemented. FIR is chosen over IIR because it’s much easier to preserve the linear phase in FIR. Although some distortions in phase likely would not cause significant problems using a machine learning model, FIR is still chosen to slightly increase model accuracy. Because the voice recognition is running on a laptop in this prototype design, an increased number of coefficients would not cause noticeably increased hardware usage or scheduling issues. However, if the final product is relying on low end, low power ARM chip to perform the tasks, IIR should be considered to reduce processing power. Comparing between different window methods including Hamming, Gaussian, and Chebyshev. Kaiser window is chosen as it offers a balance between a sharp transient and the number of coefficients needed.

The TensorFlow based voice recognition is a retrained deep speech model using customized training data instead of default training sets. The retrained model only includes a very small set of known words, including “stop”, “start”, “left” and “right”.

Other words are fed into the unknown words category and trained as noise. This retrained model with a much smaller number of words drastically increases recognition success rate. The current software divides the audio stream to 1.3 second clip to feed into the machine learning model. This length offers a balance between recognition success rate and response time. An improvement could be made on caching strategy, double buffering could be implemented so that audio would not be cut between two clips and this would increase voice recognition rate.

Navigational System Analysis

The navigational system uses an 8-bit hall-effect magnetic line tracker and a 1.5-inch magnetic strip. The magnetic tape is to be adhered to ground and line tracking sensor detects the horizontal relative location of the tape. By reading the location information into a microprocessor and using if-then logic, the speed of the two motor can be effectively controlled.

The magnetic sensor communicates serially based on a MODBUS-RTU communication protocol or by outputting the states of each of the hall-effect sensors NPN open-drain configurations. Tracking was achieved by polling each of the sensors independently. Using the internal pull-up resistors in the microprocessor, this information can be read directly through corresponding digital pins. After processing, the microprocessor outputs a 5V PWM signal, which is amplified to a nominal voltage using an integrated motor driver.

Manipulator Analysis

The manipulator implemented in the design and prototype uses open-loop control, as the lack of feedback sensors was regrettably not discovered until after

assembly and initial testing. This resulted in minor observable steady-state error in the z-direction, which was mitigated using a constant offset. The manipulator appeared to have some sort of integrated control as it traversed its range of motion in under one second without overshoot, however the joint position data was not accessible to the programmer. The manipulator has a reachable workspace consisting of a 36cm dome centered at a height of 9cm above its attached platform.

Forward Kinematics

To model the manipulator, both forward and inverse kinematic models were generated. The forward kinematics were determined based on the following DH parameters, from which a series of transformation matrices were calculated for each of the joint locations. The theta values used were adjusted such that the commanded angles inherently programmed into the controller matched the measured joint angles observed. Based on the following parameters an accurate model of the manipulator kinematics was generated using MATLAB.

Table V: HIWONDER Manipulator: DH Parameters

I	α_{i-1}	a_{i-1}	d_i	Θ_i
1	0	0	0.09	$\Theta_1 - \pi/2$
2	0	0	0	$\Theta_2 - \pi/2$
3	$-\pi/2$	0.11	0	Θ_3
4	0	0.09	0	Θ_4
5	0	0.16	0	0

Inverse Kinematics

The inverse kinematics of the manipulator were determined using an iterative algorithm called FABRIK, Forward and Backwards Reaching Inverse Kinematics developed at the Department of Engineering at Cambridge University, Cambridge, UK [11]. The algorithm is best demonstrated in the following Figure 8 . This method is far simpler than others used as it does not require matrix manipulation, instead using simple geometry. This algorithm operates by positioning the end-effector at the desired position Figure 8 (b) , drawing a line between that position and the next joint n-1, positioning joint n-1 a distance equal to the length of the link away from joint n along that line Figure 8(c), and repeating for the remaining joints Figure 8 (d). Then, the base joint is placed at its proper location Figure 8 (e). The same process repeats propagating outwards from the base towards the end effector. This cycle repeats until the base is located at its appropriate location and the end-effector is close enough to its desired position to be considered acceptable Figure 8 (f). Testing in MATLAB resulted in the end-effector being located within 0.1mm from the desired position, although higher accuracy would be possible with more iterations.

This algorithm works very well in solving planar manipulators; however, a slight modification was required to allow the algorithm to accurately model the manipulator used which is a planar manipulator with a rotating base. Using the coordinate frame of the base rather than the universal frame in this analysis resolved this issue.

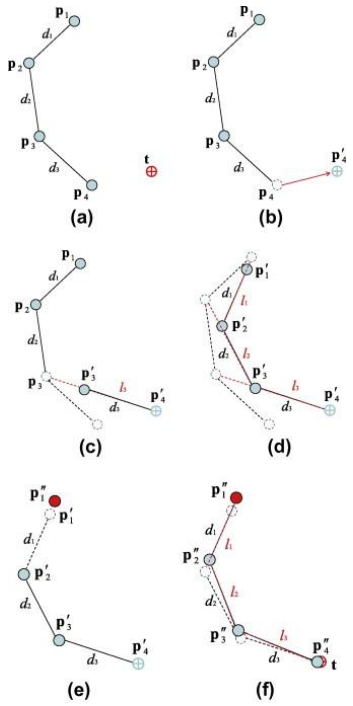

Figure 8: FABRIK Algorithm

The resolution of the manipulator is less precise than can allow for the 0.1mm accuracy determined by the FABRIK algorithm. Each joint has a resolution of 0.18º, which, during testing corresponded to an accuracy of ±0.5 cm in the x and y directions. This is also due to inherent error in the controller provided, which does not appear to account for the weight of the manipulator based on the observed steady state error in the z direction.

Design Refinement

Motor Refinement

After completing the CAD model of the chassis and manipulator, it was found that the weight of the device previously estimated to be 7 kg was inaccurate. The completed model, created from 1060 aluminum, had a mass of 10kg. After adding the weight of

fruit of 5kg, the fully-loaded robot will have a weight of 15kg. At this stage, the original gearbox motor selected was replaced with a different model which integrated a 51X reduction. This allowed the device to operate closer to its rated torque, improving its efficiency and the devices battery life. The physical dimensions of the motor were the same, as was the housing used in both models. No other modifications to the chassis construction were needed.

The motor specifications of two iterations can be found as follows:

Table VI: Drive Motor Selection Iteration

Gear Ratio	Voltage	No-load speed	Rated speed	Rated torque	No-load current	Rated current	Stall current
1:27	24V DC	325±30 RPM	230 ± 20 RPM	1.324N.m	0.3A	2.3A	7A
1:51	24V DC	172±15 RPM	122 ± 10 RPM	2.5N.m	0.3A	2.3A	7A

Storage Refinement

After the construction of collection subsystem, it was found that there was no effective way to retrieve the fruit as there is no openable door to release the container. The refinement made will be to construct an openable door at the other side that is opposite to the transmission tube entrance. To achieve full automation, a servo will be connected to the door which will open at a designated location when the robot detects the container is full. This can be done by using a pressure sensor placed at the bottom of container.

Manipulator Refinement

Based on the testing done, and the prototype construction, there are several key refinements that need to be made between the prototype and the final design. The first refinement is to install feedback sensors into the manipulator or to use a manipulator from a different manufacturer that allows for closed-loop control. In the case of the prototype, the accuracy of the manipulator was greatly improved by implementing a constant offset to the commanded position to the shoulder servo, however implementing feedback sensors would have greatly improved the design.

The end-effector was modified into a cutting mechanism that isolates and separates the tomato from its vine. This mechanism was iterated multiple times beginning as a simple claw-style gripper as was originally installed on the manipulator. The claw was modified into a scissor cutter by attaching blades to each of the grippers, due to the lack of precise control possible with the open loop control of the manipulator, this design would cause undue damage to the vine and surrounding tomatoes. Finally, the isolation cutter was developed that would encompass the tomato and cut both above and in front of the tomato simultaneously. Unfortunately, this design was not able to be fabricated due to the closure of university facilities. The scissor cutter was implemented, tested, and proven to be an effective cutting instrument; however, it lacks the safeguards of the isolation cutter.

Prototype Development

The prototype is developed to be 1:1 and fully functional, the prototype constitutes of serval subsystems including a driving subsystem, picking subsystem, collection subsystem, recognition subsystem and detachment subsystem.

Driving Subsystem

The driving subsystem is composed of two driving wheels that are mounted to DC motors, two driven wheels and an 8-bit magnetic line tracker. The line tracker will read the relative horizontal location of the magnetic strip on the ground and outputs this to a microprocessor. The microprocessor will differentiate the speed of two motors based on given information. Two 5V PWM signals are generated based on the turning scenario. The motor driver amplifies the 5V signal to 15V and sends it to each of the motors.

Collection Subsystem

The collection subsystem is integrated within the frame's built-in 300mm x 300mm x 100mm space beneath the manipulator. Three of the side panels and the base panel were fabricated from 2.5mm acrylic. The final side panel, which contained the connection interface with the transmission tube was fabricated from ½ inch plywood as the acrylic panel originally to be used was found to be too brittle to withstand the use of a 4-inch hole saw. If the panel was to be fabricated using a laser cutter, the original acrylic panel could have been used, however that service was unavailable due to the closure of university facilities. A flexible plastic tube (dryer duct) was inserted into the hole in the collection bin and connected to the manipulator end-effector using cable-ties.

Detaching & Picking Subsystem

To detach the tomato from the vine, the original end effector was modified by adding two razer blades. Thich mechanism operates similarly to garden pruners. The tomato then falls down a flexible plastic tube into the collection bin.

Figure 9: Manually Actuated Detachment Mechanism

Recognition Subsystem

The recognition subsystem uses a webcam as its the input device, the captured image is processed by MATLAB at a resolution of 640x460 to reduce processing time. The capture framerate is set to 10 frames per second for this application. Various image processing techniques were used including noise removal, RGB to binary conversion, template matching and morphological reconstruction.

Prototype Testing and Evaluation

After constructing the prototype, each of the core functions of the device were tested independently before being integrated into a single system. However, due to a lack of access to university facilities, the final system integration was unable to be completed as required connecting and mounting components could not be fabricated. What follows summarizes the tests that were completed, before and after iterations were made.

Linear Speed Test

In this test the device was fully constructed, and the linear speed of the device was measured. Between trials the average voltage applied across the driving motors was modified. The speed of the device was measured, and the battery life was estimated. The purpose of this test was to determine the performance capabilities of the device as could be directly related to its viability as an effective supplement to tomato harvesting workers. Assuming the steady-state torque applied by the motor remained consistent, the battery life at each speed was estimated as a result.

Table VII: Linear Speed Recorded Test Data

V_{nom} (V)	Duty Cycle	V_{avg} (V)	Speed (m/s)
15	30%	4.5	0.50
24	30%	7.2	0.80
10	80%	8	0.85
15	60%	9	1.00
15	100%	15	1.67

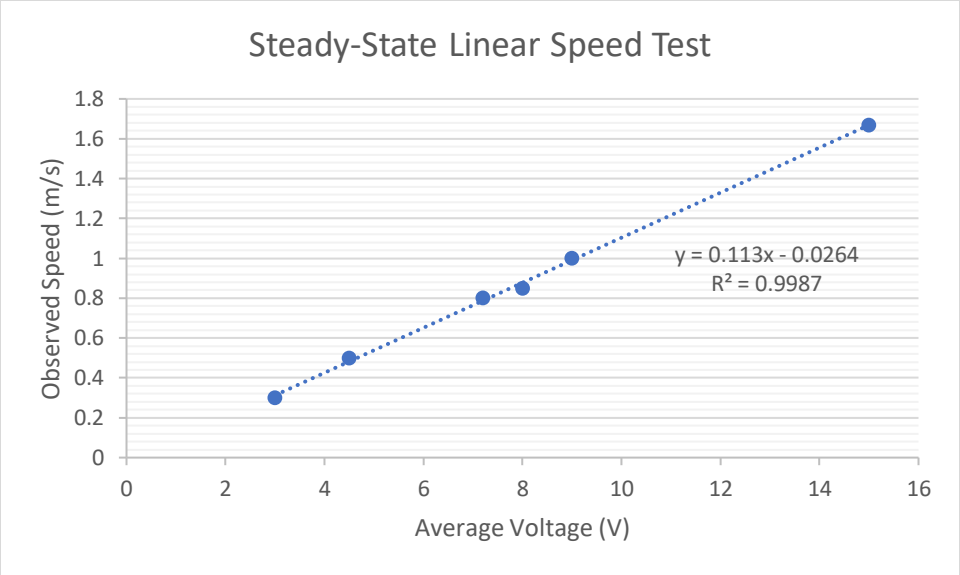

Figure 10: Steady-State Linear Speed Test Data Plotted with Linear Regression

Based on the speed data observed, the average current (which was not recorded) could be estimated along with the estimated power consumption and battery life.

Table VIII: Power Analysis and Estimated Battery Life using a 5 Ah Battery

V_{avg} (V)	Speed (m/s)	Speed (rad/s)	Torque (Nm)	Power (W)	I_{avg} (A)	5 Ah Battery Life (estimated)
3	0.30	3.34	1.98	6.61	2.20	2.27
4.5	0.50	5.56	1.98	11.01	2.44	2.05
7.2	0.80	8.90	1.98	17.62	2.45	2.04
8	0.85	9.45	1.98	18.71	2.34	2.14
9	1.00	11.12	1.98	22.02	2.45	2.04
15	1.67	18.57	1.98	36.77	2.45	2.04

Turning Speed Test

As centripetal force limits the maximum speed the device can achieve while turning, it was necessary to determine the highest possible speed the device could turn while tracking a 3 cm wide magnetic track. To conduct this test approximately 2m of magnetic track was fixed to the floor with a radium of curvature of approximately 1m. The robot was placed at the end of the track and its speed was gradually increased until the device was no longer able to follow the track. This radius of curvature was selected to represent the device reaching the end of an aisle of plants and turning to travel in the opposite direction along an adjacent aisle. Each trial was simply graded as pass/fail depending on if the robot could successfully track the magnetic strip.

Table IX: Turning Speed Test

Speed (m/s)	Pass / fail
0.30	Pass
0.50	Pass
0.80	Pass
0.85	Pass
1.00	Fail
1.67	Fail

Based on the results of the prior two tests, the device could successfully operate at a peak linear speed of 1.67 m/s and a peak turning speed of 0.8 m/s. This distinction was implemented in the navigation code to maximize the efficiency of the device

Manipulator Inverse Kinematics Testing

In the following two tests, a series of positions are commanded to the manipulator. It was during this stage of testing that it was discovered that the manipulator purchased had no feedback devices in its servos, indicating that only open-loop control was possible. This resulted in a lack of accuracy in the vertical z-direction as the device was not capable of compensating for its own weight.

Table X: Manipulator Accuracy Test Pre-calibration

Commanded Position (X, Y, Z)			Actual Position (X, Y, Z)		
25	20	20	25	20	5
20	20	20	20	20	15
10	20	20	10	20	20
-10	20	20	-10	20	20
-20	20	20	-20	20	15
-25	20	20	-25	20	5
0	0	45	0	5	40
0	10	30	0	12	25
0	15	30	0	15	25
0	20	30	0	20	25
0	25	30	0	25	30
0	30	30	0	30	20
0	35	15	0	35	10

Fortunately, this error could effectively be mitigated by adding a 10-degree offset to the shoulder motor. This had eliminated the effect of the observed discrepancy while also reducing the radial play of the motor in question.

Table XI: Manipulator Accuracy Test: Post-calibration

Commanded Position (X, Y, Z)			Actual Position (X, Y, Z)		
25	20	20	25	20	18
20	20	20	20	20	20
10	20	20	10	20	22
-10	20	20	-10	20	22
-20	20	20	-20	20	20
-25	20	20	-25	20	18
0	0	45	0	0	45
0	10	30	0	10	32
0	15	30	0	15	32
0	20	30	0	20	30
0	25	30	0	25	28
0	30	30	0	30	28
0	35	15	0	35	15

Due to the poor design of the purchased manipulator, the elbow servo overheated and ultimately burned out on two different units. This was under normal operating conditions. As a result, the reachable workspace was greatly reduced as the manipulator lost a degree of freedom. The revised DH parameters are as follows as the servo became locked in a colinear configuration with the following link.

Table XII: Revised DH Parameters After Motor Failure

I	α_{i-1}	a_{i-1}	d_i	Θ_i
1	0	0	0.09	$\Theta_1 - \pi/2$
2	0	0	0	$\Theta_2 - \pi/2$
3	-π/2	0.11	0	0
4	0	0.09	0	Θ_4
5	0	0.16	0	0

Prototype Modification and Improvements

Chassis Modifications

The original prototype was designed to test the functionality of the driving mechanism and to aid the design of the original gearbox design. Specifically, it was designed to configure the layout of the gears, shafts, bearings and other components with the integrated storage compartment and power supply. The prototype was not configurable as its replacement was, however, it was fully enclosed, waterproof, and served as an initial concept or starting point from which iterations could be made. This chassis was within budget costing approximately $40; however, it was difficult to develop further as it was constructed from acrylic.

The second and final chassis was constructed from extruded aluminum beams and cast aluminum brackets. This chassis cost approximately $115 to fabricate. The revised chassis was very configurable and simple to test as it was assembled with machine screws and aluminum brackets.

Line Tracker Modifications

In the original design and prototype, optical encoders were to be used as feedback devices for the navigation system. The rationale for this decision being their resistance to their environment, specifically their indifference to the cleanliness of the floor. However, it was suggested that this concept be modified to an external navigation system as an encoder would not be able to distinguish if a wheel was spinning freely without linear movement. This prompted the switch to a magnetic line tracking system as was implemented.

The use of individual hall-effect sensors, while proving cost-efficient was ineffective primarily due to how close they could be physically installed relative to each other (approximately 3cm apart) and their interference with each other after removing their housings to reduce this distance. The integrated magnetic line tracking sensor was used as a result

Manipulator Modifications

Based on the testing done with the manipulator, it quickly became apparent that is was only capable of open-loop control as no feedback devices were installed into any of the servos use in its construction. As a result, the observed error in the vertical direction resulting from the devices own weight could not be eliminated through closed-loop control schemes such as PID controllers. Instead, a constant offset was applied to the commanded position of the shoulder motor to counteract the radial play and steady-state error observed in prior testing. The value of this offset was iteratively modified to ensure the repeatability of the end-effector location followed a normal distribution centered about the desired position in that direction. The planar position (x/y) was consistently accurate and repeatable.

Power Electronic Modifications

Nearing the completion of the prototype construction, the two battery packs originally used were to be combined into a single pack with 15V and 7.5V supplies being separated using a simple breadboard voltage divider. This simple change was made to reduce the cost of the device and to simplify maintenance for the operator.

Image Processing Modifications

The algorithm used to identify and segment the tomatoes from the background was iteratively developed. The initial testing gave simple grayscale photos, in which the red colour was identified and highlighted. The second iteration was to create closed objects to account for oversaturation resulting from intense light. Next, the objects are identified independently and isolated as unique objects; at this stage the location of the object can referenced by the manipulator. The edges and top of the object can be determined and were intended to be used by the isolation cutter mechanism, which unfortunately was never fabricated due to the lack of access to university facilities.

Figure 11: Object Isolation Test Setup

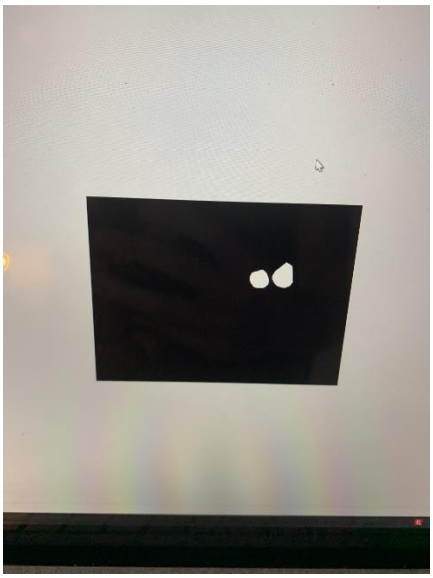

Figure 12: Object Isolation: Computer Vision Results

Overall, the image processing software was completed except the depth sensing (z-axis) part which works with ultrasonic sensor to control the manipulator's movement towards to away from the identified tomatoes. At the current stage, the image processing software can move manipulator in x-axis and y-axis (left, right, up and down), but unable to move in z-axis (towards, away) to actually perform the task.

Justification for Limited Prototype Functionality

The primary shortcoming in the prototype functionality was in the implementation of the cutting mechanism. After the design of the cutting mechanism was postponed due to a focus on the chassis and manipulator inverse kinematics, the ultimate fabrication of the mechanism was unfortunately not completed. This was ultimately a result of the lack of access to university facilities in the final weeks of the project in which the cutting mechanism, hose attachment fixture, and collection bin were to be fabricated. To fabricate these components, two pieces of equipment were required: the band saw to accurately cut acrylic, and a sheet-metal brake to create the attachment fixture. For the purposes of testing the cutting ability of the manipulator, two blades were attached to the included claw manipulator using zip ties to demonstrate the claw motor was strong enough to cut through material.

The ultrasonic sensor is not installed on the manipulator end-effector to work with the image processing software. The incomplete of ultrasonic sensor is because of two reasons: 1. The manipulator cannot support the weight of the additional ultrasonic device 2. Support structure was not fabricated to properly attach and install the ultrasonic on the end-effector. The absence of ultrasonic sensor results in image processing unable to command the manipulator to move in z-axis (depth).

During testing, it was discovered that the manipulator was poorly designed and that servo 3, the “elbow” servo, was underspecified. On two separate units this same servo burned out. Rather than disassemble, return, and reassemble a new manipulator, the same manipulator was continually used for testing with a reduced range of motion. This was to save both time and money during development. The reduction in the range

of motion predominantly effected the manipulators ability to reach a cylindrical area above its own base, it also prevented the manipulator from reaching below its base. This was accommodated for during testing when selecting commanded positions, although the workspace reduction is significant.

Resources and Budget

The following table outlines a comprehensive, itemized invoice of the material costs associated with the construction of the prototype and ultimately the final design of the fruit picking robot.

Table XIII: Itemized Prototype Fabrication Cost

Item	Quantity	Unit Cost	Total Cost
Drive wheel	2	$18.63	$37.26
Driven wheel	2	$12.61	$25.22
8-Bit magnetic line tracking sensor	1	$55.51	$55.51
BTN7971 motor driver	1	$24.09	$24.09
MD36 35W 24V DC Motor with optical encoder	2	$73.92	$147.84
Ultrasonic sensor	1	$1.32	$1.32
24V to 5V voltage converter	1	$3.20	$3.20
M5 washer	50	$0.02	$1.00
M5-12 screw	10	$0.08	$0.80
M5-14 screw	10	$0.09	$0.90
M5 – 16 screw	10	$0.09	$0.90

M5 nylon lock nut	30	$0.04	$1.20
Aluminum beam corner bracket	40	$0.53	$21.20
80cm 2020 aluminum beam	10	$1.67	$16.70
5-DOF Manipulator and associated hardware	1	$165.29	$165.29
Acrylic Panels	4	$1.10	$4.40
100 mm flexible hose	1	$2.50	$2.50
		Total	$509.89

Potential Cost Savings

Table XIV: Potential Cost Savings

Item	Cost	Savings
Reed sensor SPST	$18.00	$37.51
24V 5300RPM DC motor	$25.84	$96.15
Injection molded wheels	$10	$24.25
Total Savings		$156.11
Potential cost		$353.78

As can be seen, the project did exceed the budget by $210, this could be addressed by using single hall-effect sensors instead of the integrated sensor, using a 12V motor instead of the 24V motor specified and operating at a lower efficiency (sacrificing battery life), and at a higher average current. Savings also could have been had on the driving wheels. The wheel specified are cast aluminum, plastic wheels could have been used at the expense of durability.

Conclusions

Since the last deliverable, substantial progress had been made alongside the greatest challenges of the term as a result of the COVID-19 pandemic. The development of each of the independent subsystems was completed, although they were not fully integrated together. The final cutting mechanism, the ultrasonic mount that would allow the image processing system to achieve depth perception, nor the collection bin were fully fabricated due to a lack of access of machinery and laser cutting services.

The image processing system can successfully identify and isolate tomatoes, even if they are partially in occluded by each other, also, the edges of the tomatoes can be identified indicating the appropriate position of the isolation cutter. The manipulator was discovered to not include any feedback sensors to allow for closed loop control, and the elbow motor burnt out twice during testing. Considering this, it can accurately move to a commanded cartesian coordinate location, despite having a limited reachable workspace due to the motor failure on the prototype. The magnetic line tracking navigation system works perfectly across multiple surfaces. Given the opportunity, the missing components would be fabricated, and the independent subsystems would be integrated. In addition, more extensive testing would be done including testing on live tomato plants instead of greenhouse tomatoes, and perhaps the manipulator would have been replaced (the one selected had no datasheet or specifications provided) with a different, higher quality manipulator.

References

[1] Canadian Agricultural Human Resources Council, "Argiculture 2025: How the Sector's Labour Challenges Will Shape Its Future," Canadian Agricultural Human Resource Council, Ottawa, 2016.

[2] Canadian Agricultural Human Resources Council, "How Labour Challanges Will Shape the Future of Agriculture: Agricultural Forcast to 2029," Canadian Agricultural Human Resources Council, Ottawa, 2019.

[3] T. Sasaki, K. Iwasaki and I. Mori, "Overtime, Job Stressors, Sleep/Rest, and Fatigue of Japanese Workers in a Company," Industrial Health, 2007.

[4] A. Shikdar and Das, Biman, "The relationship between worker satisfaction and productivity in a repetitive industrial task," Applied Ergonomics, 2003.

[5] G. Kaskooli, Interviewee, *Farmworker vs Robot.* [Interview]. 17 February 2019.

[6] M. Frost, "Express," Express Newspaper, 11 October 2019. [Online]. Available: https://www.express.co.uk/finance/city/1189306/raspberry-picking-robot-fruit-veg-harvesting. [Accessed 2 Novemeber 2019].

[7] M. Dosser, H. Bischof and M. Wiltsche, "Color Blob Segmentation by MSER Analysis," in *2006 International Conference on Image Processing*, Atlanta, GA, USA, 2006 .

[8] L. L. Wang, B. Zhao, J. W. Fan, X. A. Hu, S. Wei, Y. S. Li, Q. B. Zhou and C. Wei, "Development of a tomato harvesting robot used in greenhouse," *International Journal of Agricultural and Biological Engineering,* vol. 10, no. 4, pp. 140-149, 2016.

[9] H. Heinimann, "Ground-Based Harvesting Technologies for Steep Slopes," *Proc. Int. Mountain Logging and 10th Pacific Northwest Skyline Symposium,* 1999.

[10] ASM Internation, "Properties of Wrought Aluminum and Aluminum Alloys," in *ASM Handbook, Voltume 2: Properties and Selection: Nonferrous Alloys and Special Purpose Materials*, ASM Handbook Committee, 1990, pp. 62-63.

[11] A. Arisidou and J. Lasenby, "FABRIK: A fast, iterative solver for the Inverse Kinematics problem," *Graphical Models,* vol. 73, no. 5, pp. 243-260, 2011.

[12] S. Hayashi, K. Ganno, Y. Ishii and I. Tanaka, "Robotic Harvesting System for Eggplants," *Japan Agricultural Research Quarterly,* pp. 163-168, June 2002.